ISSN: 2834-4928

Research Article

Journal of Electrical Electronics Engineering

# Research on Extracting Silicon and Iron Oxide from the Waste Ash of Mongolian Fourth Thermal Power Plant

**Yu Qian[1]*, Tungalagtamir Bold[1]*, Enkhujin Munkhtur[1], Munkhbaatar Punsantsogvoo[1] and Byambagar Batdelger[1]**

[1]*School of Applied Sciences, Mongolian University of Science and Technology, Ulaanbaatar 14191, Mongolia*

[1]*Main campus of MUST Baga toiruu 34, Sukhbaatar district, Ulaanbaatar, Mongolia*

***Corresponding Author**

1.Tungalagtamir Bold, Main campus of MUST Baga toiruu 34, Sukhbaatar district, Ulaanbaatar, Mongolia. botungalagtamir@must.edu.mn.

2. Yu Qian, Changsheng Mansion, No.29, North Xinhua Street, Xicheng District, Beiing 10003, China. npbychina@126.com.

**Submitted**: 2024, Oct 08; **Accepted**: 2024, Nov 01; **Published**: 2024, Nov 28

**Citation:** Qian, Y., Bold, T., Munkhtur, E., Punsantsogvoo, M., Batdelger, B. (2024). Research on Extracting Silicon and Iron Oxide from the Waste Ash of Mongolian Fourth Thermal Power Plant. *J Electrical Electron Eng, 3*(6), 01-15.

## Abstract

*In this research, we extracted silicon and iron oxides from the waste ash of the Mongolian fourth thermal power plant by a precipitation method. The samples were analyzed using XRD, XRF, BET, and SEM, and the following conclusions were reached. From the quantitative analysis of the chemical composition, the bottom and fly ash of the Mongolian fourth thermal power plant belong to the acid ash. The results of instrumental analysis of iron oxide obtained from the waste ash (XRF, XRD, BET, SEM), the ratio of ash to hydrochloric acid is 1:6, the hydrochloric acid concentration is 20%, the reaction temperature is 75°C, stirring speed is 250 rpm. The properties of the prepared iron oxide are the best and yield 20%, purity of 41.587%, average pore diameter of 7.5379 nm, and specific surface area of 38.87 $m^2/g$.The results of instrumental analysis of silicon dioxide obtained from the waste ash (XRF, XRD, BET, SEM) show the ratio of ash to hydrochloric acid is 1:6, the hydrochloric acid concentration is 20%, the reaction temperature is 75°C, stirring speed is 200 rpm. The yield is about 75%, the purity is 99.999%, the average pore diameter is 27.96 nm, and the specific surface area is 353.59 $m^2/g$.*

**Keywords:** Waste Ash, XRD, XRF, BET, SEM, Surface Structure

## 1. Introduction

In Mongolia, the central regional system consists of II, III, and IV thermal power plants in Ulaanbaatar city, Darkhan thermal power plant, and Erdenet thermal power plant. The ash composition from these stations varies. Coal ash is a fine ash like residue collected and captured from flue gas during heating and power generation in power plants, as well as larger particle slag (bottom ash) collected from the bottom of boilers. It is the main solid waste generated by coal fired power plants. In 2024, it is estimated that worldwide coal-fired power plants generate approximately 800 million to 1 billion tons of coal ash annually; the global utilization rate of coal ash is estimated to be approximately 60%, while the remaining 40% is disposed of in landfills [1]. The discarded coal ash causes serious problems such as water pollution, air pollution, soil pollution, and land occupation. Coal ash is often used for road backfilling, building materials, and soil improvement. Still, in recent years, with the gradual saturation of the building materials market and the improvement of agricultural soil standards, the utilization of coal ash in industries such as building materials and soil has been limited [2-4].

As of 2024, Mongolia's energy sector is predominantly coal-based, with over 90% of electricity generated from coal-fired thermal power stations [5]. Mongolia's utilization rate of coal ash remains relatively low. The country has faced challenges in effectively managing and repurposing these by-products. For instance, in 2018, the annual output of coal ash in China exceeded 550 million tons, with a utilization rate of about 70% [6-7]. In contrast, Mongolia's utilization rates have been significantly lower, primarily due to limited infrastructure, technological constraints, and a lack of comprehensive policies promoting the reuse of coal ash.

We used the waste ash from the Mongolian fourth thermal power plant as our research object. This plant produces about 330,000

tons of waste ash annually and supplies up to 30,000 tons of fine ash from electrostatic precipitators to concrete manufacturers. However, due to the limitations of the ash handling equipment and the halt of construction activities in winter in our country, the remaining ash is disposed of in an ash pond located 3 km from the plant [8]. The power station uses coal from the Baganuur and Shivee-Ovoo deposits as fuel.

**Figure 1:** Ash Pond of Mongolian Fourth Thermal Power Plant

## 2. Research of Methodology

Silicon and iron oxides were extracted from the waste ash of the Mongolian fourth thermal power plant using a precipitation method [9-11]. Figure 2 shows the scheme for the extraction of silicon and iron oxides. The experimental conditions were selected as 1:5, 1:6, 1:7, the ratio of ash and hydrochloric acid, the reaction temperature 75°C, 85°C, 95°C, and the stirring speed 150 rpm, 200 rpm, and 250 rpm, respectively.

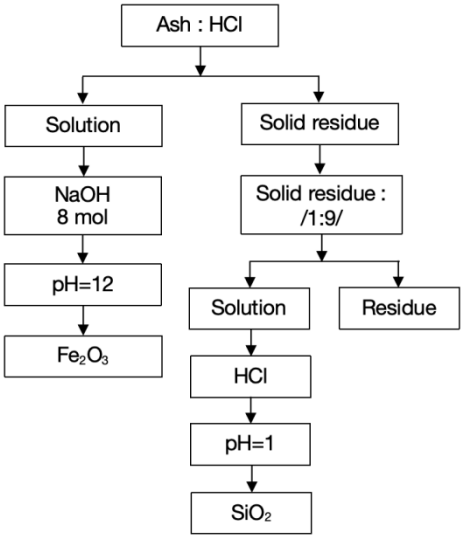


**Figure 2:** Scheme for Extracting Silicon and Iron Oxides

### 2.1. Methods of Extracting Iron Oxide

Samples and hydrochloric acid will be mixed continuously at a fixed stirring speed with the appropriate ratio at a specified temperature. After that, titrate the solution with 8 mol/l NaOH solution until the pH is 12, let it rest and filter. The filtrate is dried at 110°C to extract $Fe_2O_3$. Figure 3 shows the extracted iron oxide.

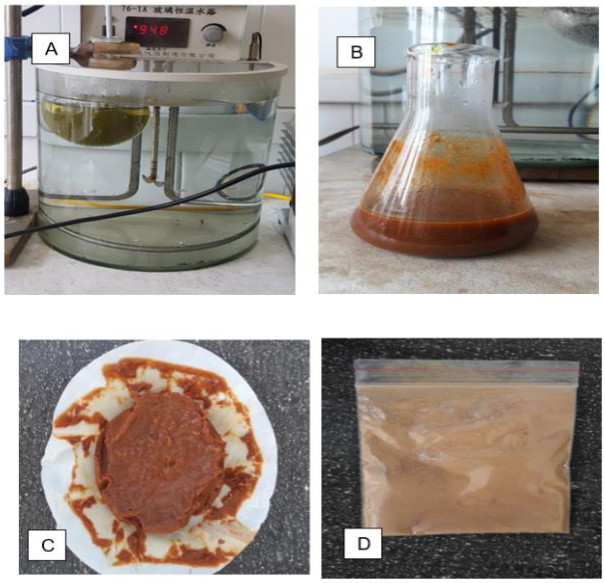


**Figure 3:** The Extracted Iron Oxide
A. Solution After Stirring at a Constant Speed B. Solution After Titration with 8 mol/L NaOH Solution,
C. Filtration of $Fe_2O_3$, D. Iron oxide

### 2.2. Methods of Extracting Silicon Oxide

The residue (precipitate) and 8 mol/L NaOH solution were taken in the 1:5, 1:6, and 1:7 ratio and stirred continuously for 5 hours in a magnetic stirrer. After that, $NaSiO_2$ is extracted with a vacuum filter, and the solution is used for further experiments. The solution is then titrated with 20% hydrochloric acid until pH=1. After that, let the solution rest for some time, rinse it thoroughly with distilled water, and filter it with a vacuum filter. The filter is dried in an oven at 110°C to remove $SiO_2$. Figure 4 shows the extracted silicon oxide.

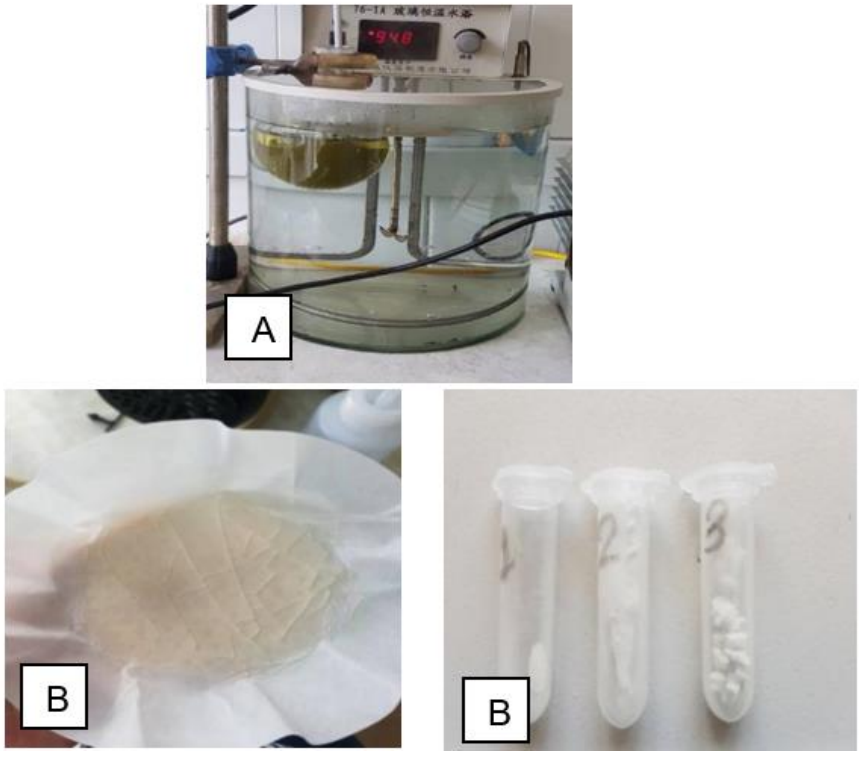


**Figure 4:** The Extracted Silicon Oxide
A. Precipitation to Extract $SiO_2$, B. Extracted Silicon Oxide

### 2.3. Instrumental Analysis Methodology

X-ray diffraction analysis: The primary X-ray tube type of the instrument is copper [Cu] anode, broad focus BF=2×20 mm, tube power 2.7 KW. The wavelength of copper anode X-rays is K_ α1=1.5406 Å. We analyzed the powder crystal samples' structure and phase using the MAXima XRD-7000 X-ray diffractometer. Measurement conditions: scattering angle range 10°~80°, angle step 3°/min. X-ray fluorescence analysis: We completed the X-ray fluorescence analysis using the HORIBA MESA-500W device. Electron microscopy: The sample's external structure, distribution, and porosity were determined using the Japanese S-3400N type electron microscope. Measurement conditions: Voltage 0.3-30 kV, working distance 5-65 mm, magnification range 5-300 K. Surface area BET: The sample's surface area and average pore diameter were determined using the ASAP-2020 device from the American company Micromeritics. Measurement conditions: Pre-treated in a vacuum environment at 200°C, nitrogen adsorption was carried out at -196°C (liquid nitrogen). Radiometric analysis: Analysis method: Conducted using gamma spectrometry.

## 3. Analysis Results of Coal and Ash Properties

### 3.1. Technical Analysis Results of Baganuur and Shivee-Ovoo Coal Deposits

Mongolian fourth thermal power plant uses coal from the Baganuur and Shivee-Ovoo deposits. Table 1 shows technical analysis results for these deposits.

| Deposits | Moisture, % | Ash, % | Volatile, % | Sulfur, % | Calories, kcal / kg |
|---|---|---|---|---|---|
| | $W^a$ | $A^a$ | $V^a$ | $S^{ad}$ | $Q^{ad}$ |
| **Baganuur** | 35.48 | 17.54 | 32.8 | 0.81 | 3580.8 |
| **Baganuur **** | 37.5 | 17.5 | 44.8 | 0.38 | 3360 |
| **Shivee-Ovoo** | 41.8 | 12.8 | 33.4 | 0.77 | 5877.83 |

[**] MNS 3818: 2001 “Technical requirements for Baganuur coal mine”

**Table 1: Results of Technical Analysis**

According to the above results, the moisture content of Shivee-Ovoo coal is 41.8%, ash content is 12.8%, volatile matter yield is 33.4%, sulfur content is 0.77%, and calorific value is 5877.83 kcal/kg. The moisture content of Baganuur coal is 35.48%, ash content is 17.54%, volatile matter yield is 32.8%, sulfur content is 0.81%, and calorific value 3580.8 kcal/kg, which is similar to MNS 3818: 2001 [12-13].

### 3.2. Results of Ash Radiation Analysis

The results of the radiation analysis of fly ash and bottom ash are shown in Table 2.

| No. | Sample name | Isotopes, Bk/kg | | | | Element content | | | Radium equivalent activity, Bk /kg |
|---|---|---|---|---|---|---|---|---|---|
| | | $^{226}Ra$ | $^{232}Th$ | $^{40}K$ | $^{137}Cs$ | U, г/тн g/tn | Th, г/тн g/tn | K, % | |
| **1** | Fly ash | 360 | 54 | 574 | <1.1 | 30 | 13 | 2 | 478 |
| **2** | Bottom ash | 142 | 41 | 738 | <1.1 | 12 | 10 | 2 | 257 |
| | **The lower detection limit (volume 0.7 L, when measured for 1 hour)** | 1.2 | 1.3 | 29.4 | 1.1 | 0.1 | 0.3 | 0.1 | - |

**Table 2 : Results of Ash Radiation Analysis**

The table below shows Mongolia's current construction and road materials radiation standards.

| No | Radium equivalent (Bk/kg) | Types of buildings and structures |
|---|---|---|
| **1** | <370 | Residential and social buildings under construction and renovation |
| **2** | <740 | Road construction and industrial buildings under construction in residential areas |
| **3** | <1500 | Roads and structures being built and repaired in uninhabited areas |
| **4** | $1500<A_{эфф}<4000$ | Roads and buildings under construction and repair: In this case, the problem will be solved with permission from the sanitary and radiation control service. |

**Table 3: Radiation Parameters for Construction and Road Materials**

Ash radiation levels are not constant. It depends on the coal seam and the characteristics of the deposit. According to the results of the radiation analysis, the equivalent activity of fly ash radium is 478 Bk/kg, and it is <740 in the standard MNS 5072: 2001 applicable to building and road materials or "Road construction and industrial buildings under construction and repair in residential areas."The radium equivalent activity of bottom ash is 257 Bk/kg and belongs to the "Apartment and social building under construction." The amount of fly ash radiation is higher than bottom ash, and some researchers have reported that the activity of coal is enriched when it is burned but that large amounts of radiation are released into the air during combustion [14].

### 3.3. Ash XRD Test Results

Figure 5 shows the analysis results of the phase composition of minerals in the fly ash and bottom ash of the Mongolian fourth thermal power plant.

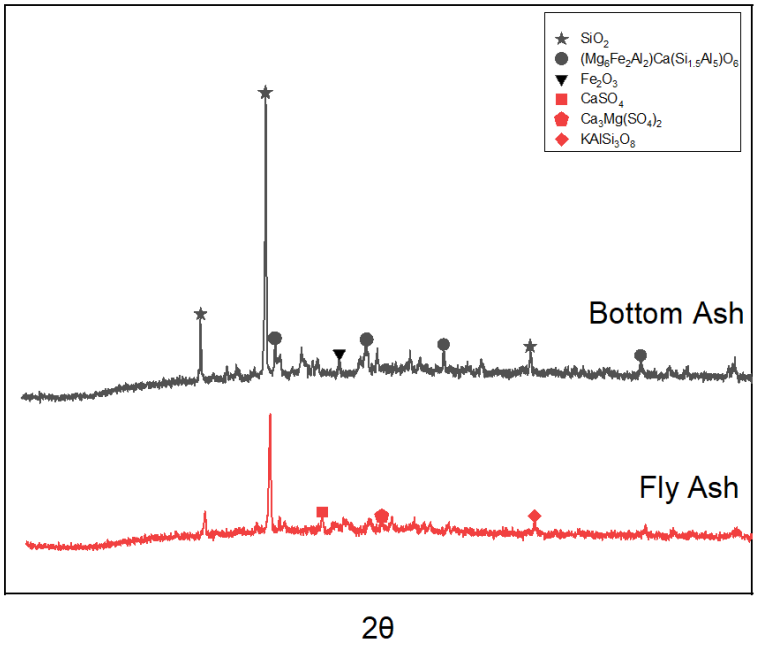


**Figure 5:** Results of X-ray Diffraction Analysis of The Fly Ash and Bottom Ash

According to the XRD analysis results, the bottom ash contained $SiO_2$-55.52%, $Fe_2O_3$-5.19%,(Mg, Fe, Ti, Al) (Ca, Na, Mg) (Si,Al )2O6-12.29%, CaO-0.35%, Ca2Mg( $Si_2O_7$) -5.53%, $NaAlSi_3O_8$ - 8.70%, $KAlSi_3O_8$ - 12.40%. However, in fly ash, $SiO_2$- -43.8%, $Fe_2O_3$-4.23%,CaO-2.73%,$K_2Ca(CO_3)_2$-5.65%,$KAlSi_3O_8$-14.91%,$NaAlSi_3O_8$-7.25%, $Ca_2Mg(SiO_4)_2$-14.33% and $CaSO_4$-7.1% were formed. In the bottom ash and fly ash, the $SiO_2$ phase (quartz) was found to occur at angles of 2θ=24.28°, 31.06°, 42.74°, 46.23°, 47.18°, 49.74°, 53.75°, 58.98° and 64.74°, and the $Fe_2O_3$ phase was found to occur at angles of 2θ=28.17°, 38.74°, 41.65°, 47.86°, 58.15° and 63.74°

### 3.4. Ash XRF Test Results

Table 4 summarizes the results of qualitative and quantitative analyses of the chemical composition of the fly ash and bottom ash samples from the Mongolian fourth thermal power plant.

| Bottom Ash | | Fly Ash | |
|---|---|---|---|
| **Oxides** | Mass (%) | **Oxides** | Mass (%) |
| **MgO** | 0.435 | **MgO** | 2.493 |
| **$Al_2O_3$** | 7.777 | **$Al_2O_3$** | 10.006 |
| **$SiO_2$** | 42.070 | **$SiO_2$** | 44.103 |
| **$SO_3$** | 2.973 | **$SO_3$** | 2.259 |
| **$K_2O$** | 1.441 | **$K_2O$** | 1.129 |
| **CaO** | 20.226 | **CaO** | 23.717 |
| **$TiO_2$** | 0.669 | **$TiO_2$** | 0.845 |
| **$Mn_2O_3$** | 0.587 | **$Mn_2O_3$** | 0.734 |
| **$Fe_2O_3$** | 22.461 | **$Fe_2O_3$** | 13.611 |
| **CuO** | 0.018 | **CuO** | - |
| **SrO** | 0.276 | **SrO** | 0.299 |
| **ZrO** | 0.055 | **$ZrO_2$** | 0.045 |

**Table 4 : Chemical Composition of Bottom Ash and Fly Ash**

According to the quantitative analysis of the chemical composition of the ash from the ash pond, most of the compounds are $SiO_2$ + $Al_2O_3$ + $Fe_2O_3$ (42.070% + 7.777% + 22.461%). And small amounts of CaO + $K_2O$ + $TiO_2$ (20.226% + 1.441% + 0.669%) were formed. In Fly ash, $SiO_2$ + $Al_2O_3$ + $Fe_2O$ compounds are formed, respectively (44.103% + 10.006% + 13.611%), as well as small amounts of CaO + $K_2O$ + $TiO_2$ compounds (23.717% + 1.129% + 0.845%).

Other researchers have suggested that the macro elements of ash be classified as acidic if the ratio of base oxides to acid oxides is less than 1 and alkaline if the ratio is more than 1. Therefore, when calculating the ratio of macronutrients from the results of the quantitative analysis of the chemical composition of bottom ash and fly ash of the Mongolian fourth thermal power plant, the ratio of macronutrients is less than 1, so it belongs to acid ash [15-16].

## 4. The Amount of Iron Oxide Extracted from the Waste Ash

This subgroup includes the iron oxide sample's phase, chemical composition, surface area, average pore diameter, surface distribution, and crystal structure.

### 4.1 XRF Results of Iron Oxide Analysis

Hydrochloric acid concentration and ash: The results of X-ray fluorescence analysis of iron oxide samples prepared with a modified hydrochloric acid ratio are shown in the table below. Test conditions: hydrochloric acid concentration: 10%, 15%, the ratio of ash to hydrochloric acid: 1:5, 1:6, 1:7. The results of X-ray fluorescence analysis of varying iron oxide concentrations and ratios are shown in Table 5.

| Sample-1 | | Sample -2 | | Sample -3 | | Sample -4 | | Sample -5 | |
|---|---|---|---|---|---|---|---|---|---|
| Oxides | Mass (%) | Oxides | Mass (%) | Oxides | Mass (%) | Oxides | Mass (%) | Oxides | Mass (%) |
| $Al_2O_3$ | 9.674 | $Al_2O_3$ | 7.596 | $Al_2O_3$ | 8.567 | $Al_2O_3$ | 7.391 | $Al_2O_3$ | 7.720 |
| $SO_3$ | 0.663 | $SO_3$ | 0.946 | $SO_3$ | 1.151 | $SO_3$ | 2.275 | $SO_3$ | 1.745 |
| CaO | 30.509 | CaO | 26.586 | CaO | 35.847 | CaO | 31.206 | CaO | 27.265 |
| $TiO_2$ | 0.722 | $TiO_2$ | 0.804 | $TiO_2$ | 0.722 | $TiO_2$ | 0.776 | $TiO_2$ | 0.819 |
| $Mn_2O_3$ | 0.548 | $Mn_2O_3$ | 1.102 | $Mn_2O_3$ | 1.085 | $Mn_2O_3$ | 1.388 | $Mn_2O_3$ | 1.166 |
| $Fe_2O_3$ | 22.926 | $Fe_2O_3$ | 28.326 | $Fe_2O_3$ | 18.949 | $Fe_2O_3$ | 19.170 | $Fe_2O_3$ | 22.604 |
| SrO | 0.329 | $SiO_2$ | 0.924 | $SiO_2$ | 1.548 | $SiO_2$ | 2.251 | $SiO_2$ | 1.512 |
| Cl | 34.629 | Cl | 33.716 | Cl | 32.131 | Cl | 34.966 | Cl | 36.691 |
| | | | | | | $K_2O$ | 0.329 | $K_2O$ | 0.299 |
| | | | | | | | | SrO | 0.178 |

Note: sample 1 -1: 5, sample 2 -1: 6, sample 3 -1: 7, sample 4- HCl-10%, sample 5-HCl-15%

**Table 5: Chemical Composition of Iron Oxide**

The above table shows that the ash to hydrochloric acid ratio was 1: 6, the hydrochloric acid concentration was 20%, and the iron oxide was 28.326%. Therefore, we selected the above conditions and used them in the following experiment.

The optimal conditions for the ash from the previous experiment were: the ratio of the ash to hydrochloric acid was 1:6, the hydrochloric acid concentration was 20%, the reaction temperature was 75°C, 85°C, 95°C, and the stirring speed was 150, 200, and 250 rpm. These conditions are based on the results of previous experiments. The results of X-ray fluorescence analysis of iron oxide with varying reaction temperature and stirring speed are shown in Table 6.

The above results show that iron, calcium, and aluminum oxides are mainly formed in the samples, and other elements are formed in small amounts. Table 6 shows the quantitative characteristics of the chemical composition of iron oxide with varying reaction temperatures and stirring rates [17].

| **Sample-1** | | **Sample -2** | | **Sample -3** | | **Sample -4** | |
|---|---|---|---|---|---|---|---|
| **Oxides** | Mass (%) | Oxides | Mass (%) | Oxides | Mass (%) | Oxides | Mass (%) |
| **$Al_2O_3$** | 14.134 | $Al_2O_3$ | 17.408 | $Al_2O_3$ | 15.911 | $Al_2O_3$ | 16.480 |
| **$SO_3$** | 1.034 | $SO_3$ | 0.804 | $SO_3$ | 1.117 | $SO_3$ | 1.113 |
| **CaO** | 45.407 | CaO | 43.978 | CaO | 38.240 | CaO | 40.517 |
| **$TiO_2$** | 1.059 | $TiO_2$ | 1.083 | $TiO_2$ | 1.097 | $TiO_2$ | 1.173 |
| **$Mn_2O_3$** | 1.842 | $Mn_2O_3$ | 1.742 | $Mn_2O_3$ | 2.048 | $Mn_2O_3$ | 1.858 |
| **$Fe_2O_3$** | 36.341 | $Fe_2O_3$ | 34.950 | **$Fe_2O_3$** | 41.587 | $Fe_2O_3$ | 38.859 |
| **SrO** | 0.184 | SrO | | SrO | | SrO | |
| **Sample -5** | | **Sample -6** | | **Sample -7** | | **Sample -8** | |
| **Oxides** | Mass (%) | Oxides | Mass (%) | Oxides | Mass (%) | Oxides | Mass (%) |
| **$Al_2O_3$** | 15.302 | $Al_2O_3$ | 14.436 | $Al_2O_3$ | 14.932 | $Al_2O_3$ | 16.436 |
| **$SO_3$** | 1.239 | $SO_3$ | 0.933 | $SO_3$ | 1.037 | $SO_3$ | 1.414 |
| **CaO** | 38.671 | CaO | 44.045 | CaO | 42.311 | CaO | 39.999 |
| **$TiO_2$** | 1.099 | $TiO_2$ | 1.157 | $TiO_2$ | 1.025 | $TiO_2$ | 1.056 |
| **$Mn_2O_3$** | 1.884 | $Mn_2O_3$ | 1.683 | $Mn_2O_3$ | 1.764 | $Mn_2O_3$ | 1.779 |
| **$Fe_2O_3$** | **41.804** | $Fe_2O_3$ | 37.746 | $Fe_2O_3$ | 38.930 | $Fe_2O_3$ | 39.315 |

**Table 6: Chemical Composition of Iron Oxide**

It can be seen from the table above, $Fe_2O_3$ is 34.950-41.804%, CaO is 38.240- 45.407%, and $Al_2O_3$ is 14.134-17.408% in the samples taken at the reaction temperature of 75, 85, 95°C and the stirring speed at 150, 200, 250 rpm. Tiny amounts of $TiO_2$ and $Mn_2O_3$ were also formed. The most suitable test conditions are sample 3, or iron oxide 41.587%, with a reaction temperature of 75°C, stirring speed of 250 rpm, and sample 5, or iron oxide 41.804%, with a reaction temperature of 85°C, stirring speed of 200 rpm [18].

### 4.2 XRD Test Results for Iron Oxide

Hydrochloric acid concentration and ash: The results of X-ray diffraction analysis of iron oxide samples prepared with a modified hydrochloric acid ratio are shown in the figure below. Test conditions: hydrochloric acid concentration: 10%, 15%, and the ratio of ash to hydrochloric acid ratio: 1:5, 1:6, 1:7. These conditions are based on the results of previous experiments.

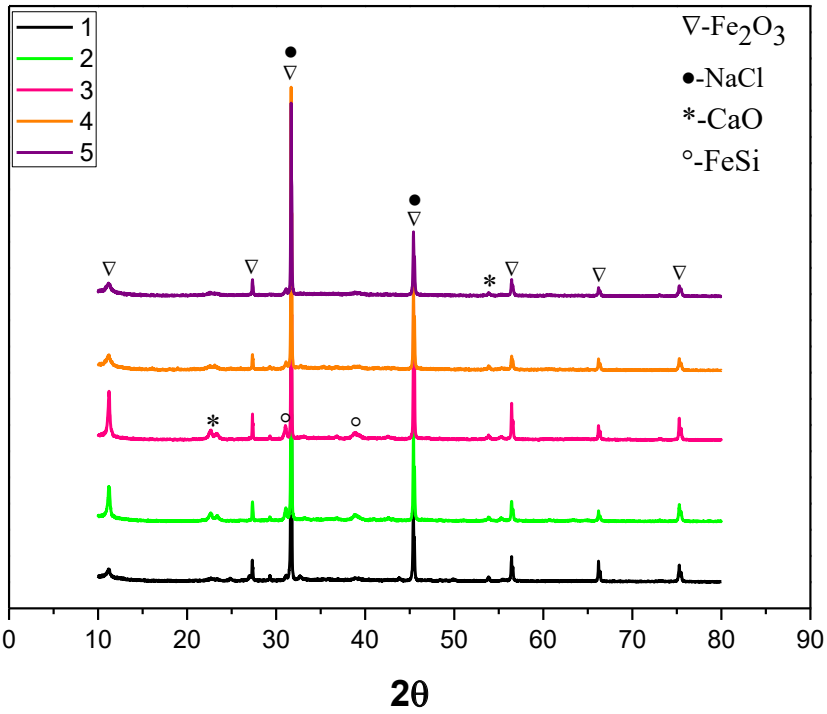


**Figure 6:** XRD Analysis of Iron Oxide with Varying Concentration and ratios of hydrochloric acid 1-1: 5, 2-1: 6, 3-1: 7, 4-HCl-10%, 5-HCl-15%

According to the results of XRD-analysis of iron oxide, the phase of $Fe_2O_3$ was formed mainly at the angles 11.19°, 27.33°, 31.54°, 45.39°, 56.39°, 66.10° and 75.13°. CaO and FeSi compounds were formed at small angles at 22.51°, 31.16°, 38.89°, and 53.79°.

### 4.3 BET Analysis Results of Iron Oxide

Hydrochloric acid concentration and ash: The results of the BET analysis of iron oxide samples prepared with varying hydrochloric acid ratios are shown in the figure and table below. We selected from the above samples to determine the pores' specific surface area and average diameter in samples 1, 2, and 5.

| No. | Sample name | Specific surface area ($m^2/g$) | Average pore diameter (nm) |
|---|---|---|---|
| 1 | $Fe_2O_3$ -1 | 8.25 | 3.936 |
| 2 | $Fe_2O_3$ -2 | 38.7 | 3.940 |
| 5 | $Fe_2O_3$ -5 | 11.3 | 3.316 |

Note: Sample 1-1: 5 250 rpm, 95°C  Sample 2-1: 6 250 rpm, 95°C  Sample 5-250 rpm, 95°C, HCl-15%

**Table 7: Hydrochloric Acid Concentration and Ash: Specific Surface Area and Average Diameter of Iron Oxide with Varying Hydrochloric Acid Ratio**

Figure 7 shows iron oxide's adsorption and desorption isotherm curves with varying hydrochloric acid concentrations and the ash to hydrochloric acid ratio.

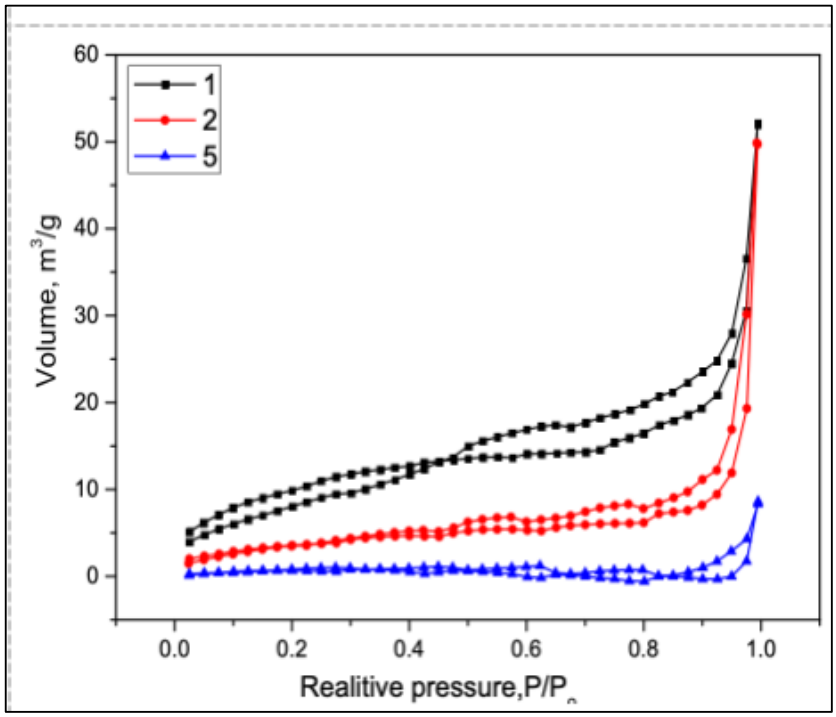


**Figure 7:** Hydrochloric Acid Concentration and Ash: Iron Oxide Adsorption and Desorption Isotherm Curves with Varying Hydrochloric Acid Ratio 1-1:5 250 rpm, 95°C, 2-250 rpm, 95°C, 5-250 rpm, 95°C, HCl-15%

As shown in Table 7, the sample-1 specific surface area is 8.25 $m^2/g^{-1}$, the average pore diameter is 3.936 nm, the sample-2 specific surface area is 38.7 $m^2/g^{-1}$, the average pore diameter is 3.940 nm, and the sample-5 specific surface area 11.3 $m^2/g^{-1}$, the average pore diameter was determined to be 3.316 nm. Hydrochloric acid concentration and ash: Iron oxide's adsorption and desorption isotherm curves with varying hydrochloric acid ratios show that type II and III adsorption curves are formed. Type II adsorption isotherm curves are standard in practice. This is called the S-type isotherm, indicating that polymolecular adsorption occurs. Type III isothermal curves belong to the type of polymolecular adsorption [19].

The results of the BET analysis of iron oxide samples prepared with different reaction temperatures and stirring rates are shown in the figure and table below.

| No. | Sample name | Specific Surface Area ($m^2/g$) | Average pore diameter, nm |
|---|---|---|---|
| 1 | 3-$Fe_2O_3$ | 38.87 | 7.5379 |
| 2 | 6- $Fe_2O_3$ | 19.02 | 5.7841 |
| 3 | 8- $Fe_2O_3$ | 10.22 | 5.4079 |

Notes: 3-75°C, 250 rpm, 6-85°C, 250 rpm, 8-95°C, 200 rpm

**Table 8: Surface Area and Average Diameter of Iron Oxide with Varying Reaction Temperature and Stirring Speed**

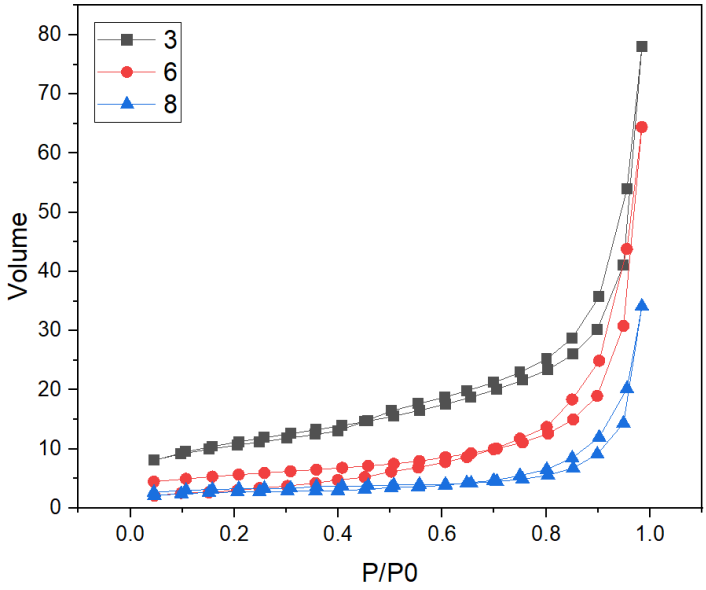


**Figure 8:** The Isotherm Curves of Iron Oxide with Varying Reaction Temperature and Stirring Speed 3-75°C, 250 rpm, 6-85°C, 250 rpm, 8-95°C, 200 rpm

Table 8 shows that the sample-3 specific surface area is 38.87$m^2/g^{-1}$, and the average pore diameter is 7.5379 nm. The sample-6 specific surface area is 19.02 $m^2/g^{-1}$, and the average pore diameter is 5.7841nm. The sample-8 specific surface area is 10.22 $m^2/g^{-1}$, and the average diameter of the pores was determined to be 5.4079nm. Iron oxide's adsorption and desorption isotherm curves with varying reaction temperatures and stirring rates show that a type III adsorption isotherm curve is formed. Type III isothermal curves belong to the type of polymolecular adsorption.

### 4.4 SEM Analysis Results of Iron Oxide

The surface structure and distribution of iron oxide prepared at a reaction temperature of 75°C, a stirring speed of 250 rpm, an ash:hydrochloric acid ratio of 1:6, and a hydrochloric acid concentration of 20% are shown in the figure below.

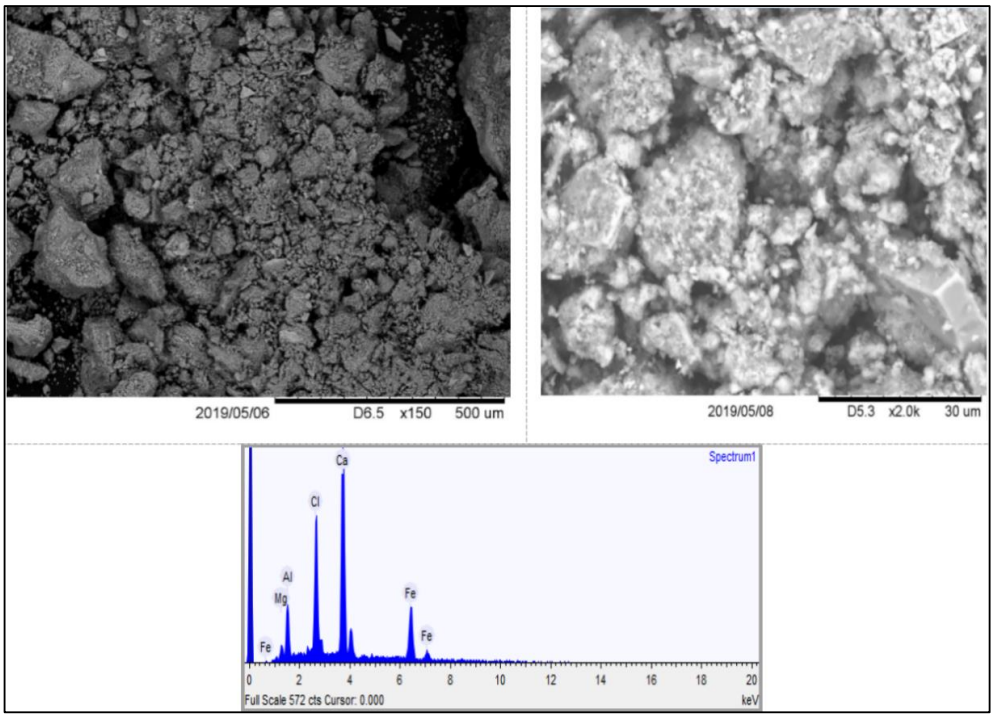


**Figure 9:** Test Results of SEM Analysis of Iron Oxide

Sample-3 reaction temperature 75°C, stirring speed 250 rpm, ash: hydrochloric acid ratio 1:6. According to the results of SEM determined under the condition of hydrochloric acid concentration of 20%, the surface structure is evenly distributed, and iron oxide, calcium oxide, and aluminum oxide are formed when shot at specific points [20,21].

## 5. XRF Test Results of Silicon Oxide

This subgroup describes the silicon dioxide sample's phase, chemical composition, surface area, average pore diameter, surface distribution, and crystal structure.

### 5.1. XRF Results of Silicon Oxide

Ash: The results of X-ray fluorescence analysis of a sample of silicon dioxide with varying hydrochloric acid ratio and hydrochloric acid concentration are shown in the figure and table below. Test conditions: ash:hydrochloric acid ratio 1: 5, 1: 6, 1: 7, hydrochloric acid concentration 10% and 15%. Table 5.1 shows the quantitative chemical composition of silicon dioxide with varying ash: hydrochloric acid ratio and hydrochloric acid concentration [22].

| Sample-1 | | Sample-2 | | Sample-3 | | Sample-4 | | Sample-5 | |
|---|---|---|---|---|---|---|---|---|---|
| **Oxides** | Mass (%) | Oxides | Mass (%) | Oxides | Mass (%) | Oxides | Mass (%) | Oxides | Mass (%) |
| **$SiO_2$** | 99.957 | $SiO_2$ | 99.973 | $SiO_2$ | 99.950 | $SiO_2$ | 99.915 | $SiO_2$ | 99.927 |
| **$Fe_2O_3$** | 0.009 | $TiO_2$ | 0.027 | $Fe_2O_3$ | 0.020 | $Fe_2O_3$ | 0.017 | $Fe_2O_3$ | 0.028 |
| **$TiO_2$** | 0.034 | | | $TiO_2$ | 0.030 | $TiO_2$ | 0.069 | $TiO_2$ | 0.045 |

Note: sample 1-1: 5 250 rpm, 95°C, sample 2-1: 6 2-250 rpm, 95°C, sample 3-1: 7 250 rpm, 95°C, sample 4-250 rpm, 95°C, HCl-10%, sample 5- 250 rpm, 95°C, HCl-15%

**Table 9: Chemical Composition of Silicon Dioxide**

The table above shows the optimal test conditions of sample 2 ash: the hydrochloric acid ratio was 1:6, and the hydrochloric acid concentration was 20%, while $SiO_2$ was 99.973% [23].

The results of X-ray fluorescence analysis of silicon dioxide samples prepared under different conditions are shown in the figure and table below. Test conditions: The reaction temperature was selected to be 75°C, 85°C, and 95°C, and the stirring speed to be 150 rpm, 200 rpm, and 250 rpm. These conditions are based on the results of previous experiments.

Table 10 shows the quantitative chemical composition of silicon dioxide samples obtained from fly ash with various parameters.

| Sample-9 | | Sample-10 | | Sample-11 | | Sample-12 | |
|---|---|---|---|---|---|---|---|
| **Oxides** | **Mass (%)** | **Oxides** | **Mass (%)** | **Oxides** | **Mass (%)** | **Oxides** | **Mass (%)** |
| $SiO_2$ | 99.974 | $SiO_2$ | 99.999 | $SiO_2$ | 99.926 | $SiO_2$ | 99.999 |
| $Fe_2O_3$ | 0.026 | $Fe_2O_3$ | 0.001 | $Fe_2O_3$ | 0.071 | $Fe_2O_3$ | 0.001 |
| **Sample-13** | | **Sample-14** | | **Sample-15** | | **Sample-16** | |
| **Oxides** | **Mass (%)** | **Oxides** | **Mass (%)** | **Oxides** | **Mass (%)** | **Oxides** | **Mass (%)** |
| $SiO_2$ | 99.973 | $SiO_2$ | 99.981 | $SiO_2$ | 99.962 | $SiO_2$ | 99.998 |
| $Fe_2O_3$ | 0.027 | $Fe_2O_3$ | 0.019 | $Fe_2O_3$ | 0.038 | CuO | 0.002 |

Note: Sample 9- $SiO_2$- 75°C 150 rpm, sample 10- $SiO_2$- 75°C 200 rpm, sample 11- $SiO_2$- 75°C 250 rpm, sample 12- $SiO_2$- 85°C 150 rpm, sample 13- $SiO_2$- 85°C 200 rpm, sample 14- $SiO_2$- 85°C 250 rpm, sample 15- $SiO_2$- 95°C 150 rpm, sample 16- $SiO_2$- 95°C 200 rpm

**Table 10: Chemical Composition of Silicon Dioxide**

From the table above, we selected 99.999% silicon dioxide for optimal test conditions at sample 10 when the reaction temperature was 75°C and the stirring speed was 200 rpm [24].

### 5.2. XRD Results of Silicon Oxide

Hydrochloric acid concentration and ash: The results of X-ray diffraction analysis of a sample of silicon dioxide prepared with a varied hydrochloric acid ratio are shown in the figure and table below. Test conditions: hydrochloric acid concentration: 10%, 15%, ash: hydrochloric acid ratio: 1: 5, 1: 6, 1: 7.

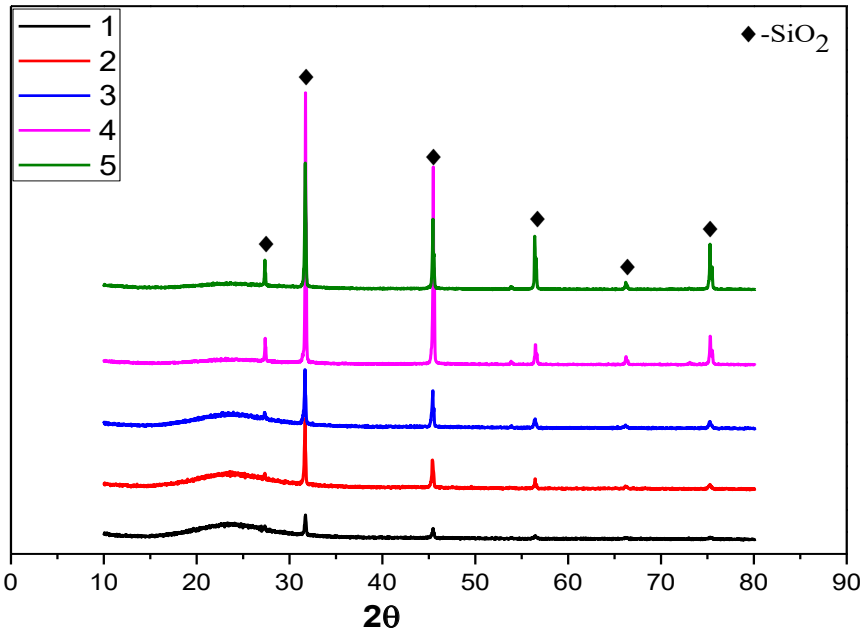


**Figure 10:** X-ray diffraction analysis of silicon oxide1-1:5 250 rpm 95°C, 2-250 rpm 95°C, 3-250 rpm 95°C, 4-250 rpm 95°C HCl-10%, 520 rpm 95°C HCl-15%

Figure 10 shows the XRD analysis of silicon dioxide, which shows that the phase of $SiO_2$ is formed at angles of 27.37°, 31.64°, 44.90°, 56.43°, 66.0°, and 75.20°.

### 5.3 BET Analysis Result of Silicon Oxide

Hydrochloric acid concentration and ash: The results of the BET analysis of a sample of silicon dioxide prepared with a varied hydrochloric acid ratio are shown in the figure and table below.

| No. | Sample Name | Specific Surface Area ($m^2/g$) | Average pore diameter (nm) |
|---|---|---|---|
| 1 | $SiO_2$-1 | 227.4 | 3.51 |
| 2 | $SiO_2$-2 | 292.6 | 3.95 |
| 3 | $SiO_2$-3 | 273.9 | 3.71 |
| 4 | $SiO_2$-4 | 179.7 | 3.511 |
| 5 | $SiO_2$-5 | 146.4 | 3.939 |

1-1:5 250 rpm 95°C, 2-1:6 250 rpm 95°C, 3-1:7 250 rpm 95°C, 4-250 rpm , 95°C HCI-10%, 5-250 rpm 95°C HCI-15%

**Table 11: Surface Area and Average Diameter of Silicon Dioxide with Varying Hydrochloric Acid Concentration and Ratio**

Figure 11 shows silicon dioxide's adsorption and desorption isotherm curves with varying hydrochloric acid concentrations and ash: hydrochloric acid ratio.

Table 11 shows that the specific surface area of sample-2 is relatively large at 292.6 $m^2/g^{-1}$, and the average pore diameter is 3.95 nm. Hydrochloric acid concentration and ash: the silicon dioxide adsorption and desorption isotherm curves with varying hydrochloric acid ratios show that the type III adsorption isotherm curve is formed. This type of isothermal curve belongs to the kind of polymolecular adsorption [25]. Figure 12 and Table 12 show the results of the BET analysis of a silicon dioxide sample prepared by varying the reaction temperature and stirring speed.

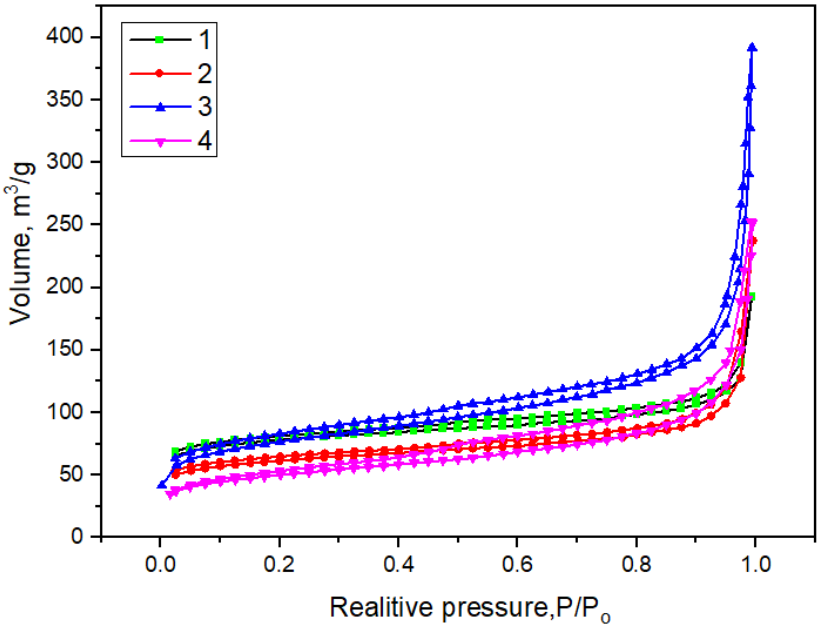


**Figure 11:** Silicon Dioxide Isothermal Curve with Varying Concentrations and Ratios Of Hydrochloric Acid

| No. | Sample Name | Specific Surface Area ($m^2/g$) | Average pore diameter (nm) |
|---|---|---|---|
| 1 | 10-$SiO_2$ | 312.35 | 32.39 |
| 2 | 13- $SiO_2$ | 353.59 | 27.96 |
| 3 | 16- $SiO_2$ | 336.02 | 51.23 |

*Note: A-75°C, 200 rpm, B- 85°C, 200 rpm, C-95°C, 200 rpm*

**Table 12: Silicon Dioxide Surface Area and Average Diameter**

Figure 12 shows silicon dioxide's adsorption and desorption isotherm curves with varying hydrochloric acid concentration and ash: hydrochloric acid ratio.

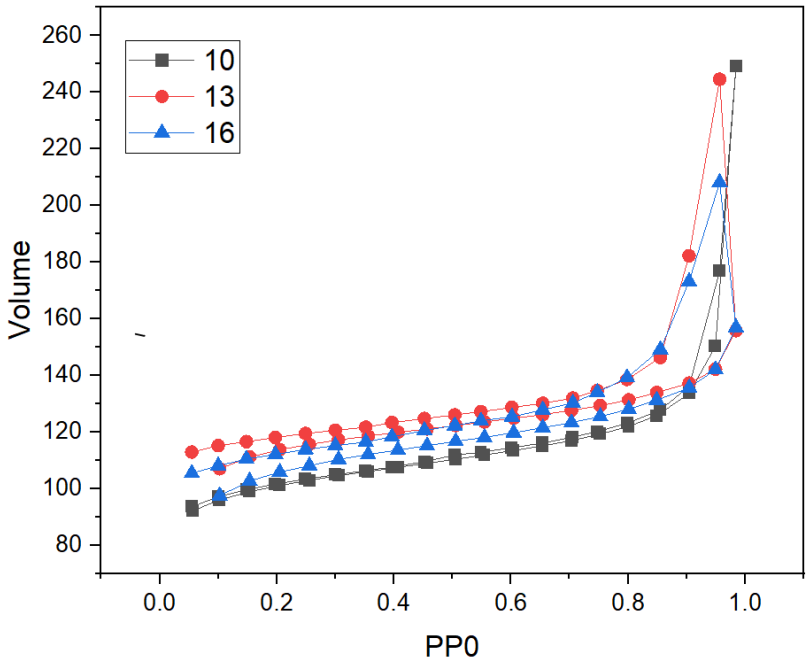


**Figure 12:** Isothermal Curve of Silicon Dioxide

Table 12 shows that sample 13's specific surface area is relatively large at 353.59 $m^2$ / $g^{-1}$, and the average pore diameter is 27.96 nm. Hydrochloric acid concentration and ash: The silicon dioxide adsorption and desorption isotherm curves with varying hydrochloric acid ratios show that a type III adsorption isotherm curve is formed. This type of isothermal curve belongs to the kind of polymolecular adsorption [26].

### 5.4 Results of SEM Analysis of Silicon Oxide

The reaction temperature is 75°C, stirring speed is 200 rpm, ash: the surface structure and distribution of silicon dioxide prepared with hydrochloric acid ratio 1:6 and hydrochloric acid concentration 20% are shown below.

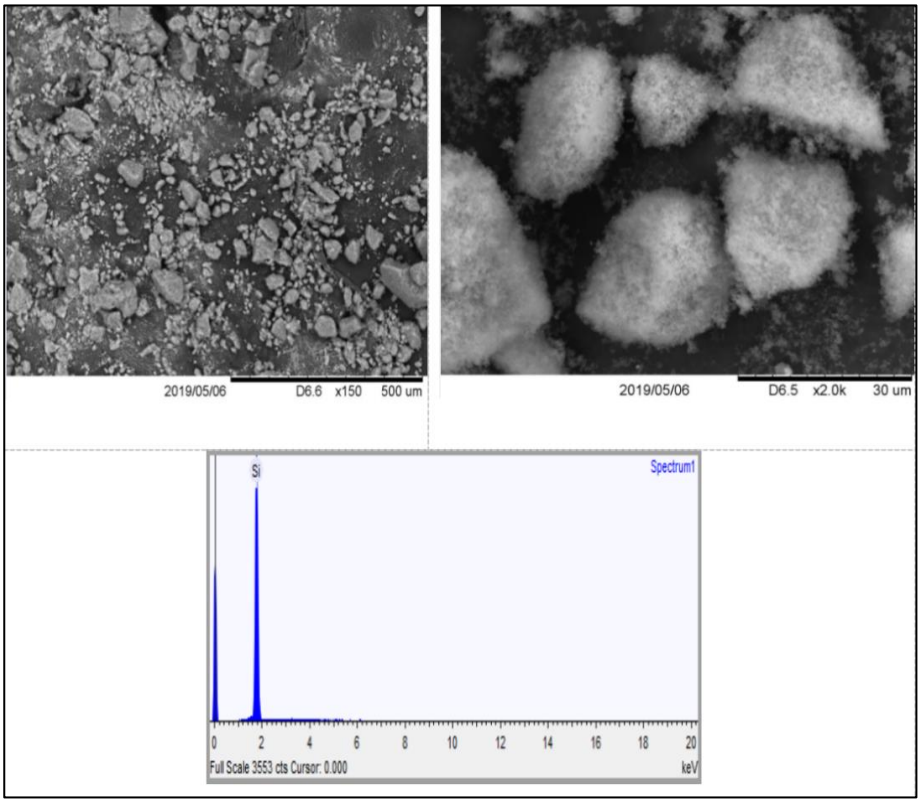


**Figure 13:** Results of SEM Analysis of Silicon Oxide

Sample-10 reaction temperature 75°C, stirring speed 200 rpm, ash: hydrochloric acid ratio 1:6, hydrochloric acid concentration 20%. This is consistent with XRF and XRD test results.

### 5.5 Determination of Silicon Dioxide and Iron Oxide Yields

We performed 26 experiments in this study to produce silicon dioxide and iron oxide under certain conditions. Table 13 shows the values determined for sample 10 (silicon oxide) and sample 3 (iron oxide) yields.

| Sample /number/ | Ash: HCl ratio | HCl concentration, % | Reaction temperature °C | Mixing speed, rpm | Yield, % |
|---|---|---|---|---|---|
| Sample-10($SiO_2$) | 1:6 | 20 | 75 | 200 | 75% |
| Sample-3 ($Fe_2O_3$) | 1:6 | 20 | 75 | 250 | 20% |

The table above shows that the yield of silicon dioxide from waste ash is 75%, and the yield of iron oxide is 20%.

**Table 13 : The Amount Determined by the Yield**

## 6. Conclusions

By precipitation, this study extracted iron and silicon oxides from the waste ash of Mongolian fourth thermal power plant. The samples were analyzed by XRD, XRF, BET, and SEM, and the following conclusions were reached. These include:

• XRD and XRF analysis of bottom and fly ash showed that hematite, quartz and calcium oxide compounds were commonly detected. Quantitative analysis of the chemical composition of the ash showed that the bottom and fly ash of the Mongolian fourth thermal power plant belong to the acid ash.

• According to the results of the radiation analysis, the radiative equivalent activity of fly ash is 478 Bq / kg and compared to the standard MNS 5072: 2001 for construction and road materials. It

belongs to <740 or "Road construction and industrial buildings under construction in place of human habitation." The bottom ash radiative equivalent activity is 257 Bq / kg and <370 for the "Renovation Housing and Public Buildings" category.

• According to the results of instrumental analysis of iron oxide obtained from the waste ash (XRF, XRD, BET, SEM), the ratio of ash to hydrochloric acid is 1:6, the hydrochloric acid concentration is 20%, the reaction temperature is 75°C, stirring speed is 250 rpm. The properties of the prepared iron oxide are the best and yield 20%, purity of 41.587%, average pore diameter of 7.5379 nm, and specific surface area of 38.87 $m^2$/g.

• According to the results of instrumental analysis of silicon dioxide obtained from the waste ash (XRF, XRD, BET, SEM), the ratio of ash to hydrochloric acid is 1: 6, the hydrochloric acid concentration is 20%, the reaction temperature is 75°C, stirring speed is 200 rpm. The yield is about 75%, the purity is 99.999%, the average pore diameter is 27.96 nm, and the specific surface area is 353.59 $m^2$/g.


## Acknowledgement

This research was supported by the Mongolian Foundation for Science and Technology (ШУТТЗ 2023/283) and (ШУТ-2021/349) projects.


## References


1. Coal Mid-Year Update July (2024). *IEA International Energy Agency.*
2. Pan, H. B., Wei, G. H., & Zhao, Z. H. (2020). Applicability analysis of comprehensive utilization of fly ash in coal-fired power plant. *Clean Coal Technology, 26*(S1), 262-267.
3. Wang, B., Li, L., Li, J., Jin, K., Zhang, S., Zhang, J., & Yan, W. (2021). Recent progresses on the synthesis of zeolites from the industrial solid wastes. *Chemical Journal of Chinese Universities-Chinese, 42*(1), 40-59.
4. Belviso, C. (2018). State-of-the-art applications of fly ash from coal and biomass: A focus on zeolite synthesis processes and issues. *Progress in Energy and Combustion Science, 65*, 109-135.
5. Dimovska, M. (2024). Mongolia's Clean Energy Transition: A pathway to sustainable and inclusive development. *United Nations Development Programme.1*.26.
6. Luo, Y., Wu, Y., Ma, S., Zheng, S., Zhang, Y., & Chu, P. K. (2021). Utilization of coal fly ash in China: a mini-review on challenges and future directions. *Environmental Science and Pollution Research, 28,* 18727-18740.
7. Temujin, J. (2017). "Properties of coal ash comprehensive processing, and application". Ulaanbaatar.
8. Hadbaatar, A., Mashkin, N. A., & Stenina, N. G. (2016). Study of ash-slag wastes of electric power plants of Mongolia applied to their utilization in road construction. *Procedia Engineering, 150,* 1558-1562.
9. Thongma, B., & Chiarakorn, S. (2019). Recovery of silica and carbon black from rice husk ash disposed from a biomass power plant by precipitation method. In *IOP Conference Series: Earth and Environmental Science* (Vol. 373, No. 1, p. 012026). IOP Publishing.
10. Gao, M., Ma, Q., Lin, Q., Chang, J., & Ma, H. (2017). A novel approach to extract SiO2 from fly ash and its considerable adsorption properties. *Materials & Design, 116,* 666-675.
11. Yadav, V. K., & Fulekar, M. H. (2020). Advances in methods for recovery of ferrous, alumina, and silica nanoparticles from fly ash waste. *Ceramics, 3*(3), 384-420.
12. Baganuur coals. (2001). Technical requirements, MONG213988, MNS 3818.
13. Narangerel, J. (2011). "Basics of Coal Chemistry and Technology". Ulaanbaatar.
14. Determination of Radioactive elements content in building materials, soil and earth crust by Gamma spectrometer's method. MONG212353, MNS 5072:2001.
15. Shan, Z., Dongyun, D., Wu, J., Daizhi. W. (2002). "The report about the comprehensive utilization of fly ash in our country." *China Academic Journal of Electric Power Environmental Protection. 5*(21),53-55.
16. Wang Peng Fei. (2006). "Review on research and development of fly ash application" China Academic. *Journal of Electric Power Environmental Protection. 2*(22),42-44.
17. Hejun, L., Qiao, L., Xiaoqing, L. (2018). Research on extracting iron oxide from ultra fine fly ash. *Bricks and Tiles [J]*, Vol.6 30-33.
18. Miao, W., Yanxia, G., Fangqin, C. (2012). Research on drawing Al and Fe from purverized fuel ash, Application Technology. No.1 Jan. Total No.216: 091-094.
19. Huaqiang, L., Runhe, Z. (2014). Extraction and comprehensive utilization of aluminum, iron and other elements in fly ash. *China Chemical Trade [J]*. Vol.16, 63-68.
20. Yanguang, C., Jia, L., Tingting, X. (2014). Study on extraction of aluminum and iron from fly ash by sodium carbonate fusion method. *Journal of Chemical Industry & Engineering*. Vol.35. No.5.
21. Clara Jeyageetha.J, Gayathri. M., Jeyapratha. J. (2020). Separation of iron oxide nanoparticles from fly ash of thermal power plant and its characterization. *International Journal of Science & Technology Research, Volume 9*, Issue 04.
22. Chengzhang, L. (2008). New technology for extraction alumina and silicone dioxide from fly ash. *Fly Ash Comprehensive Utilization. No.4*. 33-35.
23. Nzereogu, P. U., Omah, A. D., Ezema, F. I., Iwuoha, E. I., & Nwanya, A. C. (2023). Silica extraction from rice husk: Comprehensive review and applications. *Hybrid Advances, 100111.*
24. Chuanda, X., Ying, F., Zhen, L., Tao, J. Progress in extracting silicon oxide from fly Ash. *New Chemical Mateirals, Vol.41,* No.3, 158-160.
25. Yanwei, J. (2010). Experimental study on extracting silicon dioxide from fly ash. *Henan Chemical Industry. 27*(2) 53-55.
26. Wang, J. D., Zhai, Y. C., & Shen, X. Y. (2008). Study on extracting silica from fly ash by alkali leaching. *J Light Met, 12,* 23-25.